

## Shear strength characteristics of collapsed walls and influencing factors in the Benggang erosion region of Southern China

Hongyi Zhou\*, Huixia Li\*

Department of Spatial Information and Resource-Environment, Foshan University, Foshan 528000, China,  
emails: zhouhyfs@163.com (H.Y. Zhou), shelly88@163.com (H.X. Li)

Received 10 September 2018; Accepted 19 January 2019

---

### ABSTRACT

This study collected soil samples from four levels of collapsing wall soils in layers and analyzed the physical and chemical properties and strength characteristics of such soils at different layers. The results showed the following: (1) The physicochemical properties of the four layers (red soil layer, sandy soil layer, debris layer, and gravel breccia residual layer) of the collapsing wall soil are closely related to and change regularly with, the degree of weathering of the crust. (2) The effect of soil moisture on soil strength is significant. With an increase in soil moisture, the cohesion  $c$ -index of all soil layers initially increases and then decreases. (3) In the vertical section of the collapsing wall soil, the shear strength of the soil is enhanced from the bottom to the top as follows: gravel breccia residual layer < detrital layer < sandy layer < red soil layer. (4) Many physicochemical factors affect the strength of the collapsing wall soil. Only exchangeable calcium, saturated moisture content, the proportion of soil particles, and the dry density of soil particles are not significantly correlated with the shear strength.

*Keywords:* Benggang erosion; Collapsed wall; Shear strength characteristics; Granite red soil region in Southern China

---

### 1. Introduction

In the granitic areas of tropical and subtropical South China, there is a widely distributed erosional phenomenon and an associated small-scale erosional landform, which is called the “Benggang erosion” (Fig. 1) by the local people [1]. The Benggang erosion is a specific form of soil erosion in the granitic red soil region of Southern China [1,2]. The soil surface and landforms were promptly changed within the Benggang erosion by water and gravity [3,4]. Several geography scholars call the landforms formed by collapse and erosion “bad mountain landforms” and “badland landscapes.” [1]. A large amount of sediment generated by the Benggang erosion harmed farmlands, filled riverbeds, and damaged water-conserving facilities. Furthermore, mud sand flows generated from Benggang catchments may destroy roads and farmhouses and possibly result in serious

losses of life and property [5]. The Benggang erosion region is labeled as one of China’s current “ecological environment ulcers” [1]. Large-scale development within the Benggang erosion area in South China has resulted in severe soil erosion problems on the red soil hillsides in South China. “Red Deserts” are distributed within certain subtropical humid areas in the Pearl River Basin (Fig. 1), and the problem of land degradation is prominent. The erosion process in Benggang is mainly accomplished through the collapse of landform walls. Many scholars have stated that the collapse of landform walls plays a crucial role in the process of erosion; the Benggang erosion and its landforms would not have developed as they have without the collapse of landform walls. That is, collapses of landform walls are the most active part of the entire collapse process and serve as the material source for the overall movement of the Benggang erosion [4,6–8]. In the red soil region of South China, changes in the moisture

---

\* Corresponding authors.



Fig. 1. View of a typical Benggang erosion in Deqing County of Guangdong Province, China.

content of the collapsing wall soil considerably influence the shear strength, and the different levels of shear strength of soils vary with the water change law. A quantitative analysis of the change law of soil shear strength with the water content of the collapsing wall is the key to predicting soil erosion caused by collapsed walls.

Soil shear strength was found to be an important parameter in much of the literature. Dunn [9] conducted tests on samples collected from Colorado, Nebraska, and Wyoming, and he related the vane shear strength of the soil to the critical 6 tractive force, that is, the force at which erosion of the cohesive sediment began. A linear plot of the critical shear stress versus the vane shear strength was obtained in the study. Partheniades and Paaswell [10] suggested that the soil shear strength is not the only parameter used to define the erosional resistance of soil. In his experiments, Partheniades [11] reported that soils with similar strengths displayed differing critical shear stress values and that the term “critical shear stress” itself has little meaning. Partheniades [11] investigated the erosion and deposition of fine cohesive sediments in an open flume with recirculating water at ocean salinity and at a constant depth. Soil shear strength has been experimentally proven to contribute slightly in predicting soil erosion and the erosion occurrence process [12]. While shear strength is widely used in soil erosion predictions and other fields, research on the shear strength of the Benggang erosion and wall soils with water changes is limited. To date, only Zhang [13] and Lin [8] have used direct shear to analyze the magnitude and attenuation mechanism of the shear strength of Benggang erosion rock; they concluded that the shear strength of the soil reached its maximum when the soil moisture content reached 13%. However, these authors did not conduct a layered study on the shear strength characteristics of the rock and soil layers at different levels. Although the characteristics of soil strength have attracted the attention of scholars, the soil strength characteristics and influencing factors at different soil levels for collapsing wall soils (such as in this paper) have rarely been reported. In particular, the literature lacks a comparative analysis of the multilevel and varied water content changes of deep granite weathering

crust-collapsing wall soils and the physicochemical properties influencing their strength. In view of these concerns, this work measured the physicochemical properties of soil samples collected from the four layers (red clay layer, sandy soil layer, detrital layer, and gravel pebble remnant layer) of a collapsing wall soil. The strength characteristics of the different layers of soil under different water contents were measured by a shear meter, and the physicochemical factors closely related to soil strength were determined through correlation analysis. The results were used to explore the disintegration characteristics and impact factors of the collapsing wall soils and thus validate the collapsing and erosion mechanism in the region. Such validations are of considerable scientific importance in understanding the laws of collapse development and for proposing means of governance.

## 2. Materials and methods

### 2.1. Overview of study area

This study area is located in the town of Maxu, Deqing County, Guangdong Province. Deqing County (111°31′–112°15′E; 23°04′–23°30′N) is located in western Guangdong Province, on the northern shores of the Xijiang (West) River. Deqing County is located to the South of the Tropic of Cancer and has a subtropical monsoon climate, with an annual average rainfall of 1,516.5 mm, an annual average temperature of 21.5°C, and an annual average sunlight period of 1,848 h. The rocks examined in the study are biotite granite porphyry of the Yanshan Period with a weathering crust thickness of 30–60 m. Samples were collected in an active Benggang erosion area, which constituted one of the 39 total Benggang erosion areas in the region.

### 2.2. Stratification and sampling test

In the deepwater and soil conservation monitoring station of Maxu, Deqing, the author investigated the crushing degree of rock minerals and the generation of decomposed leaching and new minerals and then divided the

comprehensive profile of the weathered crust according to the characteristics of physicochemical weathering and the previous work. The granite weathering crust at the collapsing wall sampling point was divided into five levels: red clay layer (full weathered zone), sandy soil layer (strong weathered zone), detrital layer (weak weathered zone), gravel brecciated residual layer (weak weathered zone), and bedrock. From August 15, 2017, to August 18, 2017, scattered and undisturbed soil samples were obtained from the first four levels. A straight shearing cutting ring ( $\Phi 61.8 \times 20$  mm) was used to acquire the undisturbed soil to investigate the effect of moisture content on the soil strength characteristics. Five levels of water change were designed, and  $5 \times 4 = 20$  cutting ring test pieces were used for each layer of soil. (Sampling was conducted four times. One set of samples was used for bulk density and natural water content analysis, and the three remaining samples were for three runs of shear strength tests.) Four collapsing wall soil layers were collected ( $20 \times 4 = 80$  undisturbed soil samples). Each sample was numbered, wrapped in plastic wrap, and then placed in a crisper. Meanwhile, approximately 1 kg of bulk soil was obtained for physicochemical analysis. The shearing cutting ring soil samples were immediately returned and used to process the changes in soil water content in the five groups. The soil samples in Groups 1 and 2 were air-dried for 72 and 48 h, respectively, before the start of the experiment. The soil samples in Group 3 were directly measured after they were soaked in a container for 24 h. The soil samples in Group 4 were immersed in deionized water for 5 s. The surfaces of the soil samples in Group 5 were sprayed with watering cans until the water no longer infiltrated. A ZJ-4 strain-controlled direct shear meter manufactured by Hebei Hongyu Instrument Equipment Co. Ltd., (China) was used to measure the internal friction angle  $\phi$  and the cohesion force  $c$ . The shearing cutting ring soil samples were divided into three groups for repetition, and the measured results were averaged.

### 2.3. Measurement method of the physicochemical properties of collapsing wall soils

In the soil particle analysis, the soil particles with a particle diameter  $> 2$  mm were examined using the sieve analysis method, whereas soil particles with a particle diameter  $\leq 2$  mm were observed by utilizing an American Microtrac S3500 (In Foshan University) series laser particle size analyzer. Soil moisture, the dry density of soil particles, soil porosity, the soil clay elements of  $\text{SiO}_2$ ,  $\text{Al}_2\text{O}_3$ ,  $\text{Fe}_2\text{O}_3$ ,  $\text{TiO}_2$ ,  $\text{CaO}$ ,  $\text{MgO}$ ,  $\text{K}_2\text{O}$ ,  $\text{Na}_2\text{O}$ , soil pH, soil organic matter, cation exchange capacity, exchangeable calcium, free iron oxide, and alumina free exchangeable sodium were tested according to the Specifications and Methods of Soil Laboratory Analysis Project (soil classification systems research group, Nanjing Institute of Soil Science, Chinese Academy of Sciences, In Foshan University, 1991) and the Analysis of soil physicochemical properties (Nanjing Institute of Soil Science, Chinese Academy of Sciences, In Foshan University, 1978).

### 2.4. Correlation analysis

Correlation analysis refers to the analysis of two or more relevant variable elements to measure their relative

closeness. The correlation between two variables can be measured by using many statistical values, and the most commonly used value is the Pearson correlation coefficient. The calculation formula is:

$$R = \frac{1}{n-1} \sum_{i=1}^n \left( \frac{X_i - \bar{X}}{S_X} \right) \left( \frac{Y_i - \bar{Y}}{S_Y} \right) \quad (1)$$

where  $R$  is the Pearson correlation coefficient;  $n$  is the number of samples;  $X_i$  and  $Y_i$  are the values of  $X$  and  $Y$ , respectively, for the  $i$ th sample;  $\bar{X}$  and  $\bar{Y}$  are the sample mean values of  $X$  and  $Y$ , respectively;  $S_X$  represents the sample standard deviations of  $X$ ; and  $S_Y$  represents the sample standard deviations of  $Y$ . To investigate which physicochemical property had the greatest impact on the collapsing wall soil in its natural state, the study adopted the physicochemical properties of the four layers of the collapsing wall: soil ( $X$ ), the shear strength index ( $Y$ ), the internal friction angle  $\phi$ , and cohesion  $c$  under the conditions of the natural water content and the calculated Pearson correlation coefficients in Excel 2003. Each physicochemical property and shear strength index (internal friction angle  $\phi$  and cohesion  $c$ ) had three repetitions. In this study,  $n = 12$  when  $P = 0.01$  and  $R = 0.66$ . A significance correlation test was performed to identify the physicochemical factors that had significant correlations with the shear strength index (internal friction angle  $\phi$  and cohesion  $c$ ).

## 3. Research results

### 3.1. Physicochemical properties of collapsing wall soils

#### 3.1.1. Physical properties of the collapsed wall

Table 1 shows the granularity characteristics of the collapsed wall. The composition of the soil particles at all levels within the vertical section varies significantly. All fine-grained materials, such as silt and clay particles, reinforce the debris layer of the weathering crust (weakly weathered zone), which has a proportion of more than 50%. However, the amount of silt and clay particles gradually reduce from the surface of the red soil layer (fully weathered zone) to the underlying gravel and gravel brecciated residual layer (weakly weathered zone). The clay particle content decreases faster than silt. The amount of clay particles at the bottom of the gravel brecciated residual layer (weakly weathered zone) layer is only 3.58%, which is approximately 1/5 of the content of red soil. Sand content increased gradually, which comprised more than 50% of the bottom gravel brecciated residual (weakly weathered zone) layer. The changes in grain size indicate a gradual weakening of the weathering degree from the surface layer to the bottom layer.

The natural water content, soil-saturated water content, total porosity, and soil grain of the dry density of the collapsed wall are important indexes of soil structure and condition, as indicated in Table 1. Natural water content increases with depth. Saturated water content increased to a certain value and then decreased in the gravel brecciated residual layer (weakly weathered zone). The total porosity of the collapsed wall increased with depth. The density of soil particles was negatively correlated with depth.

Table 1  
Physical properties of the collapsed wall

Physical properties/layer	Red soil layer	Sandy soil layer	Debris layer	Gravel brecciated residual layer
Sand grains (2–0.02 mm, %)	29.39	32.45	45.98	52.36
Silt particles (0.02–0.002 mm, %)	53.52	51.74	46.59	44.06
Clay particles (<0.002 mm, %)	17.09	15.81	7.43	3.58
Natural water content (%)	9.93	12.43	19.72	21.56
Saturated water content (%)	33.47	33.11	34.91	27.86
Dry density of soil particles (g cm <sup>-3</sup> )	1.41	1.42	1.39	1.34
Porosity (%)	47.19	47.01	48.52	50.74
Proportion of soil particles (g cm <sup>-3</sup> )	2.67	2.68	2.70	2.72

### 3.1.2. Chemical properties of the collapsed wall

Table 2 shows that the weathering degree of the crust gradually intensifies from the bedrock to the surface. The iron oxide, alumina, and titanium oxide accumulate on the surface. The amount of these materials increases with depth. Thus, the amount of Fe<sub>2</sub>O<sub>3</sub> and Al<sub>2</sub>O<sub>3</sub> also rises, and their contents are several times higher than those at the bottom. Thus, the red soil zone is rich in iron and aluminum. However, silicon oxide, calcium oxide, magnesium oxide, potassium oxide, and sodium oxide leach; leaching intensified farther away from the surface. Significant amounts of SiO<sub>2</sub>, CaO, MgO, K<sub>2</sub>O, and Na<sub>2</sub>O were leached. The underlying contents of those materials are substantially higher than those on the surface of the red soil.

Soil pH indicates its acid and alkaline levels. Based on the vertical changes of the soil profile of the collapsed wall, acidity negatively correlates with depth. The vertical differences in soil pH values are associated with a high amount of aluminum; H<sup>+</sup>, which increases soil acidity, and Al<sup>3+</sup> exist

within the wall's soil. The degree of desilicification and allitization in the surface soil is high. Al<sup>3+</sup> increases soil acidity, and thus, the surface of the red soil has the highest acidity.

The amount of organic matter and cation-exchange capacity are important chemical properties of soils. The cation-exchange capacity initially decreases but subsequently increases as organic matter increases. The cation-exchange capacity is closely correlated with soil particle composition, the secondary clay mineral type, and organic matter. The cation-exchange capacity is generally high when clay minerals are abundant. The cation-exchange capacity in the lower part of the collapsed wall may be correlated with the high proportion of SiO<sub>2</sub>/R<sub>2</sub>O<sub>3</sub> in the soil clay minerals there. The vertical changes in organic matter are negatively correlated with soil depth because the amount of animal and plant residues is limited at greater depths.

During the transition of the granitic weathering crust of the collapsed wall from the red soil to the parent material layer of the soil, the distribution of exchangeable calcium first decreases, and then subsequently increases.

Table 2  
Chemical properties of the collapsed wall

Chemical properties/layer	Red soil layer	Sandy soil layer	Debris layer	Gravel brecciated residual layer
SiO <sub>2</sub> (g kg <sup>-1</sup> )	512.6	625.7	674.6	711.1
Al <sub>2</sub> O <sub>3</sub> (g kg <sup>-1</sup> )	278.7	227.4	155.1	134.3
Fe <sub>2</sub> O <sub>3</sub> (g kg <sup>-1</sup> )	57.1	44.9	23.4	18.9
TiO <sub>2</sub> (g kg <sup>-1</sup> )	8.1	6.6	5.6	4.8
CaO (g kg <sup>-1</sup> )	1.9	2.2	5.5	5.8
MgO (g kg <sup>-1</sup> )	0.7	0.3	4.8	6.4
K <sub>2</sub> O (g kg <sup>-1</sup> )	2.8	2.5	31.9	37.5
Na <sub>2</sub> O (g kg <sup>-1</sup> )	7.6	4.7	9.8	12.8
pH	4.36	4.45	4.91	5.22
Organic matter (g kg <sup>-1</sup> )	4.98	3.88	0.65	0.54
Cation exchange capacity (mg kg <sup>-1</sup> )	6.86	5.27	7.17	7.65
Exchangeable calcium (mg kg <sup>-1</sup> )	1.11	1.20	1.49	1.32
Exchangeable sodium (mg kg <sup>-1</sup> )	1.20	1.46	1.81	1.95
Free iron oxide (g kg <sup>-1</sup> )	1.32	1.27	1.18	0.91
Free alumina (g kg <sup>-1</sup> )	0.43	0.41	0.39	0.29

The amount of exchangeable sodium positively correlates with soil depth. Sodium is a strong cation and exhibits high chemical activity. In the hilly red soil region of South China, long-term desilicification and allitization on the surface soil cause alkali metals, such as Na and K, to leach and move. Leaching and movement intensify near the surface. However, Na<sup>+</sup>, which is found in the deep soil, has a strong ability to disperse soil. Free iron oxide and aluminum are important indexes of the degree of rock weathering. A small amount of free iron oxide and aluminum indicates a lower degree of weathering.

3.2. Change the law of the shear strength index for different soil layers of the collapsing wall

As shown in Fig. 2, a common feature of all soil layers is that the cohesion *c* index increases first and then decreases with an increase in moisture content, thereby reaching the maximum with the natural water content at approximately 26%. Cohesion *c* reaches the maximum when the soil

moisture is saturated. After saturation, the cohesion *c* of all soil layers is at the same level. The cohesion *c* of each soil layer generally changes substantially under different moisture contents. The cohesion *c* of the red soil layer decays the most, followed by the sandy layer, and then by the debris and gravel breccia residual layers. After the natural water content wetting process, the change range of the cohesion *c* index decreases with soil moisture. According to Fig. 3, the friction angle  $\phi$  in each soil layer shows an attenuation law with increasing water content. As shown in Table 3, for the different soil layers of the collapsing wall, the cohesion *c* and the internal friction angle  $\phi$  of each soil layer under different water content conditions are ranked as follows: laterite layer > sandy layer > debris layer > gravel breccia residual layer. The mean value of the shear strength index of the red soil layer is the largest, and it decreases in the subsequent soil layers. The overall trend of the shear strength change of each soil layer in this study is similar to the results of Zhang et al. [13] regarding the soil shear strength in the Benggang eroded areas in Hubei Province.

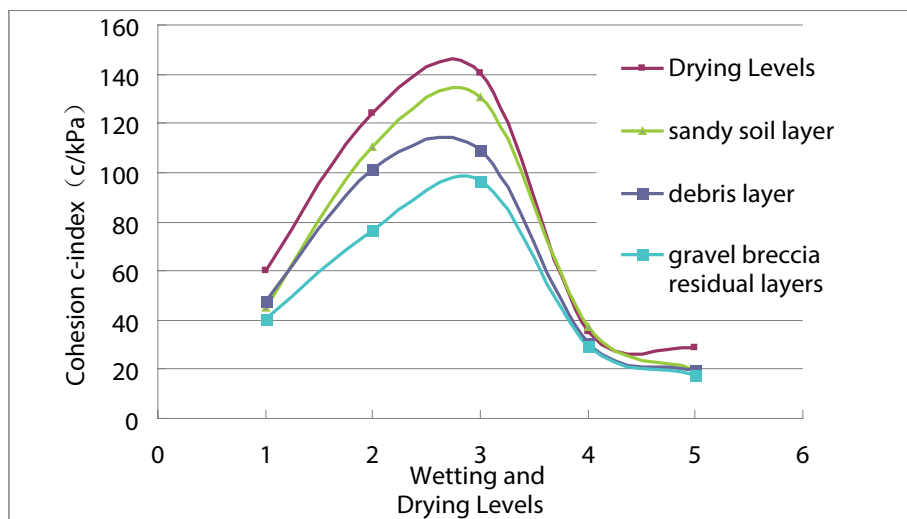


Fig. 2. Variation law of soil cohesion *c* under different soil moisture contents.

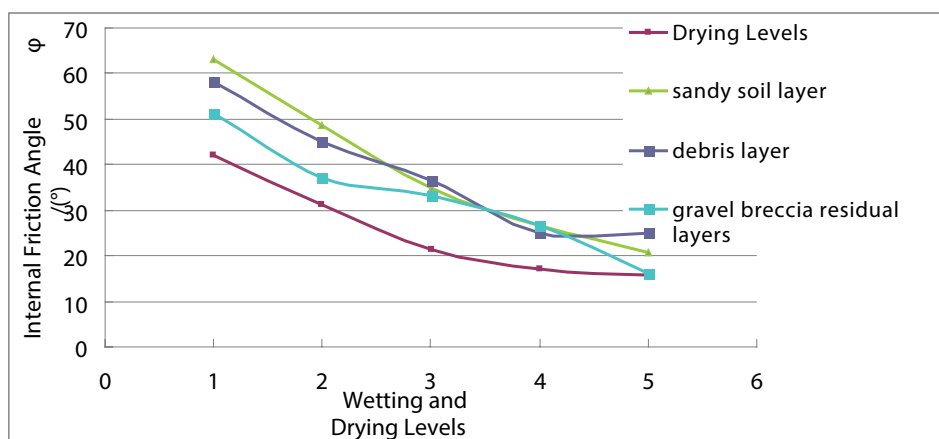


Fig. 3. Variation law of soil internal friction angle  $\phi$  under different soil moisture contents.

3.3. Analysis of attenuation characteristics of the soil shear strength index under different soil moisture contents

As illustrated in Fig. 4, the cohesion  $c$  of the collapsing wall soil sample in the study area shows a “peak value” at a moisture content of approximately 26%. Before the peak value, cohesion  $c$  positively correlates with the moisture content. After the peak value, cohesion  $c$  is extremely

negatively correlated with moisture content. This pattern contradicts those of general cohesive soils, whose cohesion  $c$  is approximately linearly reduced with a moisture content increase [13]. The trend line simulation indicates that the cohesion  $c$  and the moisture content of the soil show a pentanomial curve. The correlation coefficient  $R^2$  between cohesion  $c$  and the soil moisture content is 0.9397, which is strong for anisotropic undisturbed soil. According to Fig. 5, the internal friction angle  $\phi$  shows a negative correlation with water content. The trend line simulation reveals that the friction angle  $\phi$  and the moisture content of the soil show a pentanomial curve [15–18]. The correlation coefficient  $R^2$  between the friction angle  $\phi$  and soil moisture content is 0.7656 and has a good fitting degree. Combined with the moisture content of different treatments, the coefficient shows that the main factor index affecting shear strength is significantly different in the air-drying and the humidifying stages. Therefore, the shear strength of soil can be predicted based on soil moisture content to provide a scientific basis for the assessment of Benggang erosion stability.

Table 3  
Mean cohesion  $c$  and internal friction angle  $\phi$  of each soil layer

Layer	Cohesion $c$ (kPa)	Internal friction angle $\phi$ (°)
Drying Levels	77.788	25.58
Sandy soil layer	68.546	38.76
Debris layer	61.744	38.00
Gravel breccia residual layers	52.176	32.84

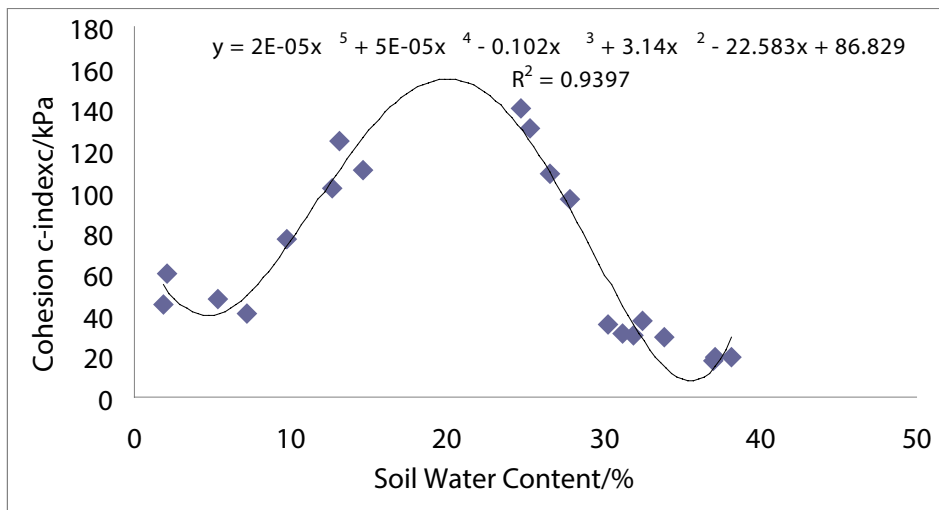


Fig. 4. Relationship between soil moisture content and cohesion  $c$ .

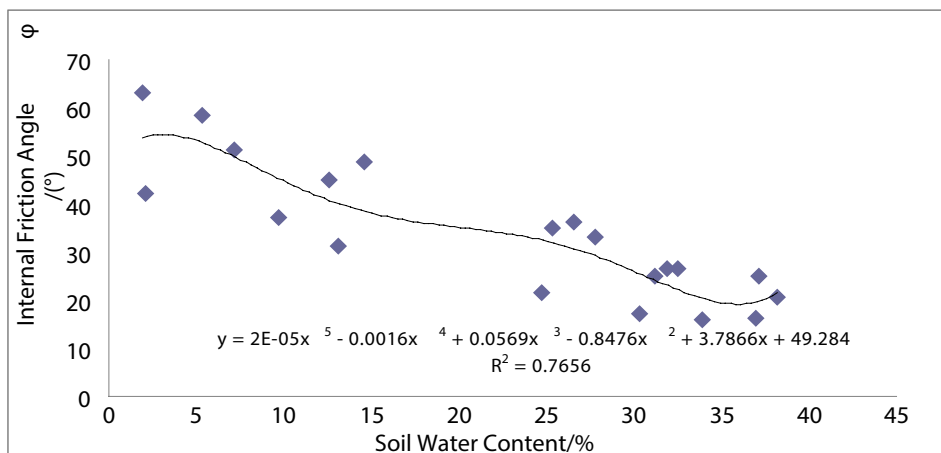


Fig. 5. Relationship between soil moisture content and internal friction angle  $\phi$ .

### 3.4. Factors affecting shear strength characteristics of collapsing wall soils

The soil shear strength index under natural water content (cohesion  $c$  and inner friction angle  $\phi$ ) and physicochemical properties were used for a correlation analysis following Formula 1 in Excel 2003. The Pearson correlation coefficient was calculated, and significant correlation tests were conducted with  $n = 12$ ,  $p = 0.01$ , and  $R = 0.66$ . The results are shown in Table 4. Most of the physicochemical properties of the collapsing wall soil have a significant correlation with shear strength. Only four factors (exchangeable calcium, saturated moisture content, the proportion of soil particles, and dry density of soil particles) are not correlated significantly to the shear resistance index. The factors that are positively correlated with the shear strength index are ranked as follows according to the correlation coefficient size: Clay particles,  $\text{TiO}_2$ ,  $\text{Fe}_2\text{O}_3$ ,  $\text{Al}_2\text{O}_3$ , Silt particles,  $\text{SiO}_2$ , organic matter, free iron oxide, and free aluminas. The factors that are negatively correlated to the shear strength index are ranked as follows according to the correlation coefficient size: sand content,  $\text{MgO}$ , natural water content,  $\text{K}_2\text{O}$ ,  $\text{CaO}$ , exchangeable sodium, pH,  $\text{Na}_2\text{O}$ , Porosity, and cation exchange capacity. The correlation coefficients show that the shear strength index, soil particle content,  $\text{Fe}_2\text{O}_3$ , and natural water content have a close relationship with the chemical composition of the clay

minerals. In the future, how these factors affect the shear strength characteristics of soils should be studied further.

### 4. Conclusions

- The physicochemical properties of the four layers of the collapsing wall soil (red clay, sandy, detrital, and gravel breccia residual layers) are significantly different, and the change in physicochemical properties is regular with the degree of weathering. The deep granite weathering shell is the material basis for the wall's collapse. The physicochemical properties of the four levels of the collapsing wall soil are the important factors determining the difference in shear strength at various levels.
- The relationship between the shear strength of each layer of the collapsing wall and the water in the vertical section of the collapsed soil shows that as the soil moisture content increases, the cohesion  $c$  of each soil layer increases first and then decreases. The internal friction angle  $\phi$  of the four soil layers is negatively correlated with water content. For the different collapsing wall soil layers under different water content conditions, the average value of cohesion  $c$  and the internal friction angle  $\phi$  of the shear strength index of each layer is in the following order: red clay layer > sandy soil layer > detrital layer > gravel pebble residual layer. For the red clay

Table 4  
Correlation analysis of the physicochemical properties of shear strength characteristics

Physicochemical properties/ shear strength characteristics	Correlation coefficient $R$ of cohesion $c$	Correlation coefficient $R$ of inner friction angle $\phi$
$\text{SiO}_2$ ( $\text{g kg}^{-1}$ )	0.87	0.89
$\text{Al}_2\text{O}_3$ ( $\text{g kg}^{-1}$ )	0.88	0.92
$\text{Fe}_2\text{O}_3$ ( $\text{g kg}^{-1}$ )	0.89	0.94
$\text{TiO}_2$ ( $\text{g kg}^{-1}$ )	0.90	0.90
$\text{CaO}$ ( $\text{g kg}^{-1}$ )	-0.98	-0.98
$\text{MgO}$ ( $\text{g kg}^{-1}$ )	-1.00	-1.00
$\text{K}_2\text{O}$ ( $\text{g kg}^{-1}$ )	-1	-0.99
$\text{Na}_2\text{O}$ ( $\text{g kg}^{-1}$ )	-0.85	-0.87
pH	-0.92	-0.91
Organic matter ( $\text{g kg}^{-1}$ )	0.80	0.79
Cation exchange capacity ( $\text{mg kg}^{-1}$ )	-0.68	-0.69
Exchangeable calcium ( $\text{mg kg}^{-1}$ )	-0.54	-0.55
Exchangeable sodium ( $\text{mg kg}^{-1}$ )	-0.93	-0.95
Free iron oxide ( $\text{g kg}^{-1}$ )	0.80	0.77
Free alumina ( $\text{g kg}^{-1}$ )	0.64	0.57
Sand grains (2–0.02 mm, %)	-1.00	-1.00
Silt particles (0.02–0.002 mm, %)	0.88	0.88
Clay particles (<0.002 mm, %)	0.95	0.93
Natural water content (%)	-0.98	-0.96
Saturated water content (%)	0.49	0.47
Dry density of soil particles ( $\text{g cm}^{-3}$ )	0.55	0.53
Porosity (%)	-0.74	-0.72
Proportion of soil particles ( $\text{g cm}^{-3}$ )	-0.39	-0.37

layer, which has a high clay content, the shear strength is high within a certain range as water content increases. This characteristic explains why the collapsing wall does not collapse easily under strong short and light rainfall intensities, under which conditions the water content of the collapsing wall soil, especially the red clay layer in its upper part, does not quickly degrade the threshold of cohesion. Consequently, the soil is strong and does not easily collapse. However, under continuous rainfall conditions, the water content of the soil also continues to increase. Once the water content reaches approximately 26%, the cohesion of the soil decreases sharply. The internal friction angle also decreases, thus resulting in a reduction of soil shear strength and subsequent wall collapse. For the sandy, detrital, and gravel breccia residual layers, the cohesion is low and mainly relies on the internal friction angle to resist external forces. The shear strength is low due to the lack of cement between the soil particles. Therefore, once the landform's erosion cuts into its sandy, debris, and gravel breccia residual layers, the developing rate of the erosion is greatly increased, thereby intrinsically causing the collapse of the landform.

- Most of the physicochemical properties of the collapsing wall's soil have a significant correlation with the shear strength index. The factors that are positively correlated with the shear strength index are ranked as follows according to the correlation coefficient size: Clay particles,  $\text{TiO}_2$ ,  $\text{Fe}_2\text{O}_3$ ,  $\text{Al}_2\text{O}_3$ , silt particles,  $\text{SiO}_2$ , organic matter, free iron oxide, and free aluminas. The factors that are negatively correlated to the shear strength index are ranked as follows according to the correlation coefficient size: sand content,  $\text{MgO}$ , natural water content,  $\text{K}_2\text{O}$ ,  $\text{CaO}$ , exchangeable sodium, pH,  $\text{Na}_2\text{O}$ , porosity, and the cation exchange capacity. The correlations between shear strength and exchangeable calcium, saturated moisture content, the proportion of soil particles, and dry density of soil particles are the only ones that are not significant. The sizes of the correlation coefficient show that the shear strength index is closely related to the soil structure factor and the chemical content of clay minerals. In future research, the content and morphology of secondary clay minerals should be tested further to analyze how dispersive sodium and cemented calcium and clay minerals affect shear strength.

## 5. Discussion

The physicochemical properties of the collapsing wall soil and the shear strength test show that the soil in the lower part of the collapsing wall (detrital and gravel breccia residual layers) is not completely broken due to the weathering of quartz, feldspar, and other minerals. The particles are remarkably coarse and lack organic matter, the free iron oxide and aluminum contents are low, and a lack of cement material is observed between the soil particles. Consequently, the soil below the collapsing wall is loose, easily disintegrates in water, and has a low soil strength. Combined with our previous study, this work reveals that the upper part of the collapsing wall soil (red clay and sandy layers) is more prone to crack than the lower part and that the development of crack is more substantial than that in

the lower soil (detrital and gravel breccia residual layers). Therefore, when rainfall occurs, rainwater penetrates the lower soil easily through cracks. During and after rainfall, the infiltration of water and the water flow along the erosion wall caused the exposed wall soil layers to swell and disintegrate, and the soil strength was low. At this time, the bottom gravel breccia residual layer is the most likely to disintegrate and be transported by the water flow, thereby leaving the overlying red clay layer and sandy soil suspended and thus contributing to the wall's collapse. This finding also verifies the phenomenon observed in the field from one side. In other words, once the red clay layer, which has a small thickness, is destroyed and eroded by runoff, the wall's collapse will be difficult to control, and the collapse speed will increase by multiples. Therefore, in the process of Benggang erosion management, special attention should be paid to protecting the laterite layers from destruction. In the lower part of the collapsing wall soil (debris and gravel breccia residual layers), the shear strength is low, the soil is easily disintegrated by water, and the void surface of the soil on the upper part of the collapsing wall becomes suspended. In the lower part of the collapsing wall, the soil shear strength is reduced due to the rainfall, and the collapse and digging → result from the water mean → suspended soil is formed → collapse → continued deep digging. This cycle continues, and the collapse continues to occur until the heads of all directions approach or reaches the watershed, the edge of the collapsing land and the collapsing pile form a stable gradient, and the bottom of the channel forms a balanced profile. Therefore, the effect of the physicochemical properties of the collapsing wall soil on disintegration, infiltration, and soil strength must be studied to provide a scientific basis for further elucidating the causes of collapse and erosion, thereby further enriching the theories of collapse and erosion and allowing for the adoption of effective prevention and control measures.

## Acknowledgment

This work is supported by the project of the National Natural Science Foundation of China entitled "The impact of development of soil cracks in collapsed walls on wall collapsing stability in granite red soil region of South China" (No. 41371041), the project of the National Natural Science Foundation of China entitled "Impact of rocky desertification on stand transpiration of *Zenia insignis* plantation and the mechanism" (No. 41401108).

## References

- [1] J.X. Xu, Benggang erosion: the influencing factors, *CATENA*, 27 (1996) 249–263.
- [2] A. Ahmed, A. Nasir, S. Basheer, Ground water quality assessment by using geographical information system and water quality index: a case study of Chokera, Faisalabad, Pakistan, *Water Conserv. Manage.*, 3 (2019) 7–19.
- [3] S.-h. Luk, P.D. diCenzo, X.Z. Liu, Water and sediment yield from a small catchment in the hilly granitic region, South China, *CATENA*, 29 (1997) 177–189.
- [4] T. Xiaoling, M.A. Ashraf, Z. Yanyan, Paired observation on light-cured composite resin and nano-composite resin in dental caries repair, *Pak. J. Pharm. Sci.*, 29 (2016) 2169–2172.
- [5] L. Xuqing, L. Yayun, L. Chao, Z. Li, Y. Hao, F. Chao, M.A. Ashraf, Identification of residual non-biodegradable

- organic compounds in wastewater effluent after two-stage biochemical treatment, *Open Life Sci.*, 11 (2016) 396–401.
- [6] Y. Liang, D.H. Ning, X.Z. Pan, D.C. Li, B. Zhang, Benggang erosion feature and control in Southern red zone, *Soil Water Conserv. China*, 1 (2009) 31–34.
- [7] M.T. Naidu, D. Premavani, S. Suthari, M. Venkaiah, Assessment of tree diversity in tropical deciduous forests of Northcentral Eastern Ghats, India, *Geol. Ecol. Landscapes*, 2 (2018) 216–227.
- [8] J.S. Lin, Y.H. Huang, M.-K. Wang, F.S. Jiang, X.B. Zhang, H.L. Ge, Assessing the sources of sediment transported in gully systems using a fingerprinting approach: an example from South-East China, *CATENA*, 129 (2015) 9–17.
- [9] I.S. Dunn, Tractive resistance of cohesive channels, *J. Soil Mech. Found. Div., ASCE*, 85 (1959) 1–24.
- [10] E. Partheniades, R.E. Paaswell, Erodibility of channels with cohesive boundary, *J. Hydraul. Div., ASCE*, 96 (1970) 755–771.
- [11] E. Partheniades, Erosion and deposition of cohesive soils, *J. Hydraul. Div., ASCE*, 91 (1965) 105–138.
- [12] Z.F. Wu, J.Z. Wang, Relationship between slope disintegration and rock-soil characteristics of granite weathering mantle in South China, *Res. Soil Water Conserv.*, 14 (2000) 31–35.
- [13] X.M. Zhang, S.W. Ding, C.F. Cai, Effects of drying and wetting on nonlinear decay of soil shear strength in slope disintegration erosion area, *Trans. Chin. Soc. Agric. Eng.*, 28 (2012) 241–245.
- [14] M. Kamal, R. Younas, M. Zaheer, M. Shahid, Treatment of municipal waste water through adsorption using different waste biomass as activated carbon, *J. CleanWAS*, 3 (2019) 21–27.
- [15] H.Y. Zhou, H.X. Li, Q. Ye, G.W. Wu, Simulation of morphological development of soil cracks in the collapsing hill soil region of Southern China, *Res. Soil Water Conserv.*, 23 (2016) 338–342.
- [16] Z. Zainuddin, A.M. Kamil, In-vitro regeneration of *Orthosiphon Stamineus* (Misai Kucing) using axillary bud, *Sci. Heritage J.*, 3 (2019) 8–10.
- [17] A. Alsulaiman, A. Al Nizam, Evaluation ability of different barada river *Micrococcus* spp. strain to bioremediation of hydrocarbons, *J. CleanWAS*, 2 (2018) 1–5.
- [18] X.L. Liu, D.L. Zhang, Temporal-spatial analyses of collapsed gully erosion based on three-dimensional laser scanning, *Trans. Chin. Soc. Agric. Eng.*, 31 (2015) 204–211.
- [19] E. Partheniades, Erosion and deposition of cohesive soils, *J. Hydraul. Div., ASCE*, 91 (1965) 105–138.
- [20] Y. Rajendran, R. Mohsin, Emission due to motor gasoline fuel in reciprocating lycoming O-320 engine in comparison to aviation gasoline fuel, *Environ. Ecosyst. Sci.*, 2 (2018) 20–24.
- [21] Y.M. Reznik, Influence of physical properties on deformation characteristics of collapsible soils, *Eng. Geol.*, 92 (2007) 27–37.
- [22] A.A. Omar, M.S. Hossain, M.M. Parvin, Study on knowledge, attitude and practices towards the solid waste management in Karan District, Mogadishu Somalia, *Environ. Contam. Rev.*, 1 (2018) 22–26.
- [23] X.M. Zhang, S.W. Ding, C.F. Cai, Effects of drying and wetting on nonlinear decay of soil shear strength in slope disintegration erosion area, *Trans. Chin. Soc. Agric. Eng.*, 28 (2012) 241–245.
- [24] M.H. Mahtab, M. Ohara, M. Rasmy, The impact of rainfall variations on flash flooding in Haor areas in Bangladesh, *Water Conserv. Manage.*, 2 (2018) 6–10.
- [25] H.X. Chen, F.H. Li, S.L. Hao, Effects of soil water content and soil sodicity on soil shearing strength, *Trans. Chin. Soc. Agric. Eng.*, 23 (2007) 21–25.